POLITECNICO DI TORINO
Repository ISTITUZIONALE

Mitigation of human-induced lateral vibrations on footbridges through walkway shaping

Original
Mitigation of human-induced lateral vibrations on footbridges through walkway shaping / Venuti, F., Bruno, L.. - In: ENGINEERING STRUCTURES. - ISSN 0141-0296. - 56:(2013), pp. 95-104. [10.1016/j.engstruct.2013.04.019]

Availability:
This version is available at: 11583/2507917 since:

Publisher:
Elsevier

Published
DOI:10.1016/j.engstruct.2013.04.019

Terms of use:

This article is made available under terms and conditions as specified in the corresponding bibliographic description in the repository

Publisher copyright

(Article begins on next page)

13 October 2026

Mitigation of human-induced lateral vibrations on footbridges through walkway shaping

Fiammetta Venuti[a,*], Luca Bruno[a,*]

[a] *Politecnico di Torino, Department of Architecture and Design, Viale Mattioli 39, I-10125, Torino, Italy*

Abstract

In the last decade, the issue of human-induced lateral vibrations on footbridges has attracted an increasing interest due to the construction of several lightweight and flexible structures, which are highly sensitive to dynamic pedestrian action. A new approach to the mitigation of human-induced lateral vibrations on footbridges is proposed. The approach develops from the analogy between crowd- and wind-structure interaction phenomena. The mitigation measure addresses the passive control of the crowd flow and the applied force in turn, in analogy to aerodynamic countermeasures already adopted in Wind Engineering. Crowd flow control is accomplished by shaping the walkway in plan, in order to modify the pedestrian density, speed and walking frequency. A simplified approach to the preliminary assessment of the footbridge and to the conceptual design of the modified walkway is first proposed. A detailed computational analysis is subsequently applied to a test-case to evaluate the effectiveness of the proposed approach.

Keywords: footbridges, human-induced lateral vibrations, mitigation measures, walkway shaping, crowd flow control

Nomenclature

b	variation of the walkway width
B	width of the walkway
B_0	initial width of the walkway
$\mathscr{C}$	damping operator
D	Dynamic Amplification Factor
F	amplitude of the modal force
f_{pp}	force component due to pedestrians synchronized among each other
f_{ps}	force component due to pedestrians synchronized to the structure
f_{s}	force component due to uncorrelated pedestrians
f_{z}	pedestrian lateral force per unit length
g	gravity acceleration
$g(\tilde{\dot{q}}_z)$	function that models the reduction of the walking velocity due to the deck motion
G	average pedestrian mass
L	length of the footbridge span
$\mathscr{L}$	stiffness operator
m_c	crowd mass per unit length
m_r	ratio of the crowd to structure mass
m_s	structure mass per unit length
M	modal mass

*Corresponding author. Tel: (+39) 011.090.4880
Email address: fiammetta.venuti@polito.it (Fiammetta Venuti)

n_{pp}	pedestrians synchronized among each other per unit length
n_{ps}	pedestrians synchronized to the structure per unit length
n_s	uncorrelated pedestrians per unit length
$\mathbf{q}$	structural displacement
$\ddot{q}_{z,\mathrm{lim}}$	perception threshold of the lateral acceleration of the deck
$\ddot{q}_{z,M}$	maximum lateral acceleration of the deck
$\tilde{\ddot{q}}_z$	envelope of the lateral acceleration of the deck
$\ddot{Q}_z$	amplitude of the steady state modal acceleration
t	time variable
v	walking velocity
v_M	free walking velocity
w	average width occupied by a walking pedestrian
w_0	average lateral width of the human body
x	space variable along the footbridge longitudinal axis
y	space variable along the footbridge vertical axis
z	space variable along the footbridge lateral axis
α	Dynamic Load Factor of the first harmonic of the pedestrian force
γ	exponent of the speed-density relation
$\varphi(x)$	mode shape
ρ	pedestrian density
ρ_{c}	critical density below which synchronization does not take place
ρ_{ca}	capacity density
ρ_{in}	incoming crowd density
ρ_{lim}	limit density that induces a lateral acceleration equal to $\ddot{q}_{z,\mathrm{lim}}$
ρ_M	maximum crowd density
$\rho_{M,0}$	initial value of the maximum crowd density
ω_{pl}	lateral step circular frequency
ω_r	ratio of the lateral step frequency to the structure frequency
ω_s	natural circular frequency of the structure
$\omega_{s,0}$	natural circular frequency of the empty footbridge
ζ	damping ratio

1. Introduction

The issue of human-induced vibrations on footbridges has become one of the leading research topics in structural dynamics during the last decade. This is due to the recent trend towards increased slenderness and reduced mass, stiffness and damping. Among others, the problem of lateral vibrations induced by synchronized pedestrians - the so-called Synchronous Lateral Excitation (SLE) - has especially attracted the attention of researchers after the closure of the London Millennium Footbridge in 2000 [1]. The SLE phenomenon can occur on any footbridge with a lateral frequency around 1 Hz and crossed by a sufficient number of pedestrians. The SLE is due to the development of synchronization phenomena that enlarge the lateral vibrations until the pedestrians stop walking because they are no longer able to maintain balance (for a review, see [2, 3, 4]).

SLE can be ascribed to flow-structure interaction phenomena, such as the ones involving wind and structures, e.g., Vortex-Induced Vibrations (VIV) and lock-in: the air flow around long-span bridge decks, chimneys and tall buildings in VIV is replaced by the crowd flow along the footbridge in SLE. Crowd and wind streams differ in several key aspects: pedestrians are active agents while air particles are not; crowd flow is compressible and in some circumstances shows granular features, while wind flow is incompressible and turbulent in civil engineering applications. Despite these differences, the occurrence of synchronization and self limitation of the cross-flow structural response is common to the behaviour of both coupled systems. This analogy has inspired some authors to adapt models widely used in VIV analysis to SLE. Examples of experimental (see for instance [5, 6]), analytical (e.g., [7]) and computational [8] models can be found in the literature. To the best of the authors' knowledge, the VIV-SLE analogy has never been

systematically exploited to adapt the full range of VIV mitigation measures to SLE.

In general, the reduction of the flow-induced structural response can be obtained by acting on one of the two components of the coupled system: on the structure, in order to reduce its response by varying its dynamic properties, or on the flow in order to modify/suppress the source of excitation.

Mitigations on the structural side disregard the particular kind of flow (e.g., wind [9, 10] or crowd [2, 11]), while they are adapted to the structural typology and the structural response threshold value at which they should be effective. In the case of ligthweight and slender footbridges, mitigations generally consist of adding extra damping, since increasing the mass or the stiffness implies high costs and undesired aesthetic impact. Most of the footbridges that have experienced SLE have been subsequently provided with passive dampers such as viscous dampers [1], friction dampers [12], Tuned Mass Dampers [13, 14] or Liquid Mass Dampers [15].

Mitigations on the flow side strongly depend on the kind of flow to be modified, so that measures conceived for a kind of flow (e.g., wind) cannot be directly transferred to another one (e.g., crowd flow) or *vice versa*. However, they can serve as a source of inspiration. The conceptual design of these mitigations requires a deep phenomenological understanding and modelling of the source of excitation as well as the structural behaviour. A sufficient scientific background has been recently acquired in the field of Wind Engineering, so that a number of aerodynamic devices are presently employed to reduce wind-induced vibrations. Several examples of applications to tall buildings [10, 16] and long-span bridges [17, 18] can be found in the literature. They are based on the shaping of the overall structure (e.g., elicoidal shape of tall buildings) or on the introduction of punctual elements (e.g., guide vanes around bridge decks). Crowd flow control strategies have been proposed in the fields of applied mathematics, physics and transportation engineering (see e.g., [19, 20]), thanks to the development of dynamic models in which the pedestrians are treated as a dynamic system rather than a simple source of load. The control of crowd flow, e.g., in pedestrian traffic or evacuation scenarios, is often accomplished by punctual obstacles (e.g., columns) located in strategic positions, in order to force the crowd flow to follow certain patterns and avoid the formation of jams or ease evacuations (see for instance [21, 22]). However, to the authors' knowledge crowd control strategies have never been systematically applied to the mitigation of structural vibrations on footbridges, except for the recent suggestion in [23], where temporary barriers along the footbridge path are expected to modify the crowd flow and to reduce the footbridge response in turn.

This work proposes a strategy of crowd flow control based on the smooth widening/narrowing of the walkway width along the span of the footbridge, with the aim of controlling the structural response. Such a proposal requires a modelling approach where the crowd is not described as a simple load applied to the structure, but as a dynamic system which interacts with the structure.

The paper develops through the following Sections: in Section 2 a simplified criterion is proposed to allow the footbridge designer to predict the most suitable shaping strategy, and it is applied to four real world test-cases; in Section 3 the effectiveness of the mitigation measure is assessed more precisely by means of the crowd-structure interaction model previously developed by the authors [24]; Section 4 describes the application of the approach to an ideal footbridge, while the conclusions and research perspectives are outlined in Section 5.

2. Conceptual design of the mitigation measure through a simplified approach

The proposed mitigation measure is based on the walkway narrowing/widening along the footbridge span. The measure is expected to affect the crowd density, and consequently the walking velocity and step frequency, i.e., the load exerted by the pedestrians on the structure. Specifically, the walkway narrowing/widening is set with the aim of reducing the bridge lateral acceleration under its perception threshold value $\ddot{q}_{z,\mathrm{lim}} = 0.1$ m/s^2 [25]. As a consequence, synchronization between the pedestrians and the structure does not take place also for incoming crowd density $\rho > \rho_{\mathrm{lim}}$, where ρ_{lim} is the density which induces a lateral acceleration equal to $\ddot{q}_{z,\mathrm{lim}}$ [26] on the footbridge in the initial geometrical configuration.

Two remarks should be made. First, the proposed mitigation measure is expected to be ineffective in the so-called unconstrained walking regime, where few pedestrians sparse along the walkway do not interact among each other. Second, a variation of the walkway width can induce a variation of the deck stiffness and of the lateral frequency in turn. In this study, the structural properties do not vary, in order to isolate, discuss and evaluate only the effects of the mitigation measure on the crowd-induced load.

In this Section a simplified criterion for the preliminary assessment of an existing structure and/or the conceptual design of a mitigation measure is proposed. The criterion is conceived to help the footbridge designer to predict the

most suitable shaping strategy. The criterion is, then, applied to four real world footbridges to evaluate its general applicability.

2.1. Simplifying assumptions

The criterion is based on four simplifying assumptions (SA), which allow the complexity of the SLE phenomenon to be reduced.

SA 1: walkway shaping

The modified walkway width B is constant along the span L and equal to:

$$B = B_0(1 + b/B_0), \tag{1}$$

where B_0 is the original value of the walkway width and b is the width variation. Even if every feasible value of b can be adopted in the proposed approach, reasonable bounds are:

- if $b < 0$ (walkway narrowing), $\max(|b|) = B_0 - 2w$, where $w = 1.62w_0$ is the average lateral width occupied by a walking pedestrian, being $w_0 = 0.45$ m the average lateral width of a human body [30]. In other words, two pedestrians are allowed to walk side-by-side in the narrowest section of the walkway;
- if $b > 0$ (walkway widening), $\max(|b|) = B_0$, that is, the walkway width double in the widest configuration.

SA 2: crowd density and velocity

Because of the constant walkway width and in the absence of crowd-structure interaction, the stationary crowd density is homogeneous along the span and can be approximated as:

$$\rho = \rho_{\text{in}}\, B_0/B = \rho_{\text{in}}/(1 + b/B_0), \tag{2}$$

where ρ_{in} is the expected density at the footbridge inlet. In other terms, the crowd density ρ along the widened/narrowed footbridge is assumed to be proportional to the geometric expansion/contraction ratio B_0/B of the walkway. The values of practical interest of the incoming density ρ_{in} are in the range $[\rho_{\text{lim}}\ \rho_{\text{ca}}]$, being ρ_{ca} the capacity density [31] corresponding to the watershed between free and congested crowd behaviour. Indeed, if $\rho_{\text{in}} < \rho_{\text{lim}}$ lateral oscillations are not perceived and the footbridge does not require mitigation measures. Moreover, the scenario $\rho_{\text{in}} > \rho_{\text{ca}}$ is not a realistic in-service condition for most of the footbridges which experienced crowd events in the literature.

The crowd walking velocity is known to be affected by crowd density, as widely observed in the pedestrian dynamic literature (e.g., see the review in [31]): the higher the density, the lower the walking velocity. This velocity-density relation is expressed by the so-called fundamental law. The one proposed by Weidmann [32] and revisited in [30] is adopted in the following:

$$v = v_M \left\{1 - \exp\left[-\gamma\left(\frac{1}{\rho} - \frac{1}{\rho_M}\right)\right]\right\}, \tag{3}$$

where ρ_M is the maximum density at which pedestrians stop walking and v_M is the free walking velocity of the unconstrained pedestrian. Both ρ_M, v_M and the free parameter $\gamma = \bar{\gamma}\rho_M$ are sensitized to the geographic area and travel purpose by means of fitting to experimental data [30]. Some examples of fundamental laws for Europe and different travel purposes are graphed in Fig. 1a. It can be observed that the law provides a non linear but continuous dependence of the walking velocity on the crowd density. In particular, the law clearly accounts for the unconstrained walking regime, where the walking speed is not affected by variation of the crowd density ($\rho \leq 0.3$ ped/m^2).

SA 3: force model

If the modification of the walkway width is effective, the resulting lateral acceleration remains below the lock-in threshold and the pedestrians do not synchronize to the structure. This assumption, together with SA 2, allows a simplified force model to be adopted [26]. The lateral force per unit length exerted by a crowd of density ρ is given by the contribution f_{pp} of the n_{pp} pedestrians synchronized among each other and the contribution f_s due to the remaining n_s uncorrelated pedestrians:

$$\mathrm{f}_z = \mathrm{f}_{pp} + \mathrm{f}_s. \tag{4}$$

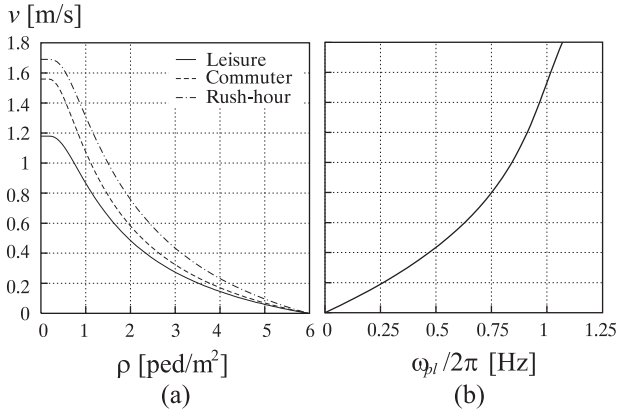

Figure 1: Pedestrian fundamental laws (a) and frequency-velocity relation (b)

The above mentioned numbers of pedestrians per unit length are defined as:

$$\begin{aligned} n_{pp} &= \rho B\, S_{pp} \\ n_s &= \rho B - n_{pp}, \end{aligned} \tag{5}$$

where S_{pp} is the synchronization coefficient which accounts for the synchronization among the pedestrians. Its dependence on the crowd density is expressed through the data-fitting-based law:

$$S_{pp}(\rho) = \begin{cases} 0 & \rho \le \rho_c, \\ 1 - \exp\left[-8.686(\rho - \rho_c)/\rho_M\right] & \rho > \rho_c, \end{cases} \tag{6}$$

with $\rho_c = 0.6$ ped/m^2 the critical density value below which syncronization does not take place. The two force components are expressed as:

$$\mathrm{f}_{pp} = n_{pp}\alpha G g \sin(\omega_{pl} t), \tag{7}$$

$$\mathrm{f}_s = 1/L\sqrt{n_s L}\,\alpha G g \sin(\omega_{pl} t), \tag{8}$$

where α is the Dynamic Load Factor (DLF) of the first harmonic of the force, $G = 70$ kg the average pedestrian mass, g the gravity acceleration, ω_{pl} the lateral circular step frequency. Several studies have been directed to the measurement of the DLFs of the pedestrian force (e.g. summarized in [27]). Herein, the value $\alpha = 0.04$ proposed by [28, 29] is retained. The lateral step frequency is expressed as a function of the walking velocity v (Eq. 3) through the equation

$$\omega_{pl} = \pi(2.93v - 1.59v^2 + 0.35v^3), \tag{9}$$

which best fits experimental data in the literature (Fig. 1b, for more details, see [30]). The relation between ω_{pl}, v and ρ is shown in Figure 1.

SA 4: Structural response

One mode is assumed to mainly contribute to the structural response, so that the latter can be estimated solving the single-degree-of-freedom modal equation of the mode of interest. The amplitude of the steady-state modal acceleration is given by the well-known expression:

$$\ddot{Q}_z = \frac{F}{M} D, \tag{10}$$

where the amplitude of the modal force F, the modal mass M and the Dynamic Amplification Factor D are given by:

$$F = \alpha G g \left[\rho B S_{pp} + \sqrt{\rho B \frac{(1 - S_{pp})}{L}}\right] \int_0^L \varphi(x)dx \tag{11}$$

$$M = (m_s + m_c) \int_0^L \varphi(x)^2 dx \tag{12}$$

$$D = [(1 - \omega_r^2)^2 + (2\zeta\omega_r)^2]^{-0.5} \tag{13}$$

$\varphi(x)$ being the mode shape. The overall mass per unit length is expressed in a simplified form as the sum of the structural mass m_s and of the crowd mass $m_c = \rho GB$, as suggested in [25]. ζ is the damping ratio and $\omega_r = \omega_{pl}/\omega_r$ the ratio of the lateral step frequency to the structure frequency. The latter can be derived as:

$$\omega_s = \omega_{s,0} \frac{1}{\sqrt{m_r + 1}}, \tag{14}$$

where $\omega_{s,0}$ is the natural circular frequency of the empty footbridge and m_r is the crowd to structure mass ratio. It should be noticed that all the terms of Eq. (10) depend on the two design variables ρ_{in} and b through Eq.s (1)-(2)-(4)-(9)-(14).

2.2. Application to four real footbridges

The lateral acceleration $\ddot{Q}_z$ is evaluated as a function of ρ_{in} and b for a sample of four real footbridges, which have shown problems of human-induced lateral vibrations. Their structural and crowd parameters (Table 1) cover a sufficiently wide range of values, in order to allow general considerations to be outlined. The footbridges are ordered for decreasing structural mass and walkway width. It is worth pointing out that the M-bridge represents a limit case due to its extreme slenderness (L/B_0) and lightweight (m_s and $m_{r,\max}$).

Figure 2 plots the dependence of the parameters which affect the lateral acceleration, i.e., the modal force, modal

Table 1: Crowd and structure parameters for four real footbridges

Footbridge	L [m]	B_0 [m]	$\omega_{s,0}/2\pi$ [Hz]	ζ %	m_s [kg/m]	$m_{r,\max}$	ρ_M [ped/m^2]	v_M [m/s]	$\bar{\gamma}$
Solferino [33]	106	13.5	0.71	0.4	4900	1.16	6	1.18	0.245
T-bridge [15]	179	5.25	0.93	1.13	4200	0.67	7.7	1.48	0.273
Millennium bridge [1]	108	4	0.80	0.7	2000	0.84	6	1.18	0.245
M-bridge [34]	320	1.5	1.025	0.27	600	1.35	7.7	1.04	0.245

mass and frequency ratio, on the design variables ρ_{in} and b. A general trend can be observed for all footbridges: the modal force F increases for increasing value of ρ_{in} and decreasing value of b, while the frequency ratio ω_r has the opposite trend; the modal mass M is independent from b and linearly increases with ρ_{in}.

The resulting steady state acceleration is plotted in Fig.s 3(a)-(d): the black curves on the 3D surfaces are the iso-contours corresponding to the lock-in threshold $\ddot{q}_{z,\text{lim}}$. The iso-contours are also plotted in the $\rho_{\text{in}} - b$ plane in Fig.s 3(e)-(h): the gray areas correspond to the comfort zones, that is, the values of ρ_{in} and b that assure the lock-in threshold is not exceeded. As expected, the trend of $\ddot{Q}_z$ and of its limit iso-contours is similar for all the footbridges, except for the M-bridge: the latter is, in fact, so narrow that only a walkway widening could be considered.

2.3. Derivation of the verification/design criterion

Looking at the diagrams of Fig.s 3(e)-(g), a general verification/design criterion can be outlined. For any given footbridge a diagram similar to the one sketched in Fig. 4 can be derived and used both as a verification and design/retrofitting chart. In the first case (red dashed curve), for the original walkway width ($b = 0$), the analyst can read in the chart the limit value of crowd density $\bar{\rho}$, abscissa of the intersection between the limit curves and the $b = 0$ line. If the expected incoming crowd density in service ρ_{in} is above $\bar{\rho}$, the comfort requirements are not fullfilled, i.e., ρ_{in} induces a perceptible lateral acceleration on the original footbridge. In this case, the chart can be used for design/retrofitting purposes (green dash-dot curve): the designer can read the limit values $\bar{b}$ and $\underline{b}$, ordinate of the intersection between the limit curves and the ρ_{in} vertical line. The absolute value and sign of $\bar{b}$ and $\underline{b}$ orient the designer towards the choice of the most suitable shaping strategy. In the example sketched in Fig. 4, $|\underline{b}| < |\bar{b}|$ and $\underline{b} < 0$, so that walkway narrowing is expected to be more effective than widening in reducing the lateral acceleration below the lock-in threshold.

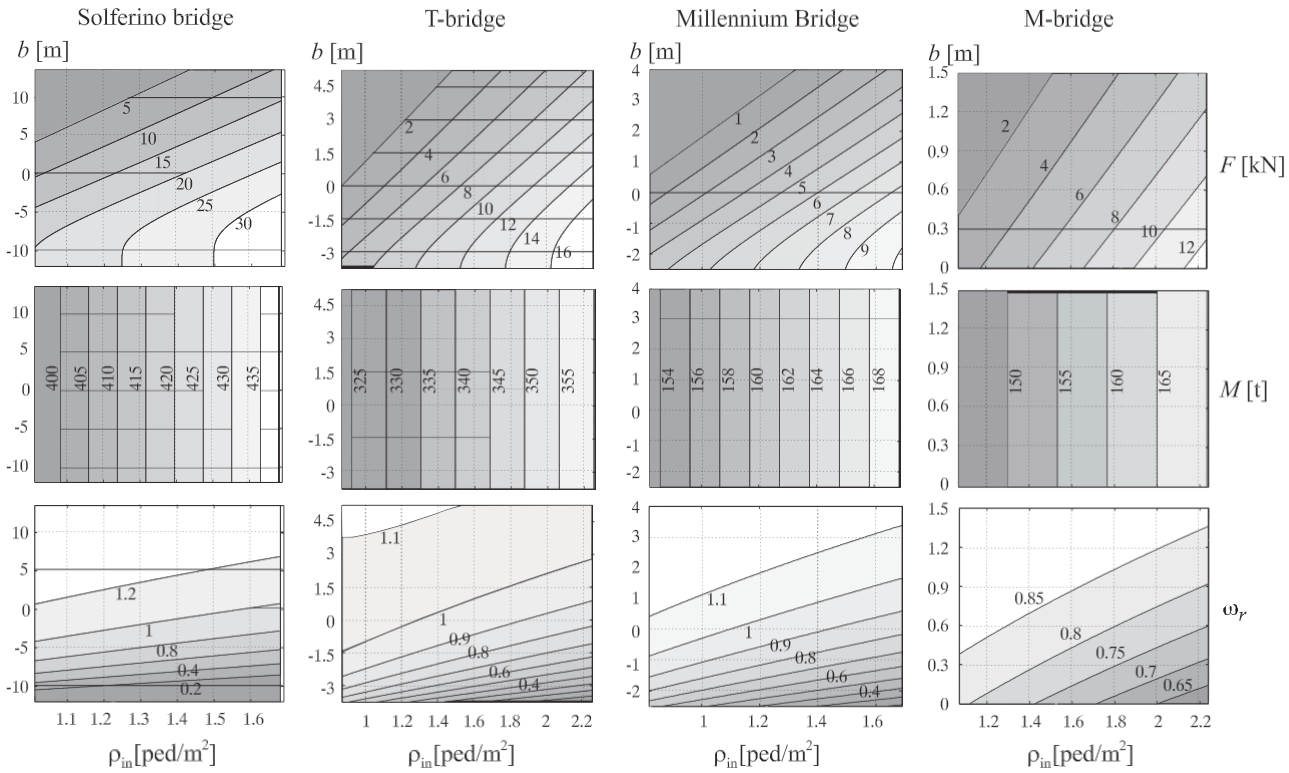

Figure 2: F (first row), M (second row) and ω_r (third row) in the $\rho_{in} - b$ plane for the four footbridges

3. Detailed design and analysis through the Crowd-Structure Interaction (CSI) model

The criterion discussed in the previous section, due to the simplifying assumptions upon which it relies, is intended as a preliminary tool to orient the designer towards the most suited sizing strategy of the walkway width. In the subsequent design steps, a refined model can meet further design needs, in particular: i. to allow handling more flexible shaping strategies of the walkway, e.g., a walkway width which varies along the span; ii. to evaluate more precisely the efficiency of the proposed mitigation measure. On the one hand, variable width may be required by planning conditions or recommended for structural reasons. For instance, the walkway width at abutments cannot vary or the walkway narrowing/widening can obey to a single (or several) selected mode shape(s) to specifically affect the corresponding modal force(s). On the other hand, crowd density, velocity and walking frequency are expected to be no longer homogeneous in the x direction for variable width. Hence, a modelling approach which fully accounts for the effects of SLE and variable walkway on the crowd flow is recommended. In the following, reference will be made to the CSI model previously proposed by the authors in [24]. The model is based on the partitioning of the coupled system into two subsystems, the Crowd (C) and the Structure (S), and on the two-way interaction between them (Fig. 5). Specifically, the crowd behaviour (i.e., the walking velocity) is affected by the structural response and the latter is affected by the crowd through the force model and the crowd added mass.

The detailed model is brefly described in the following four subsections, which represent the counterpart of the four simplified assumptions described in the previous Section, in the sense that each assumption is removed and the model generalization is highlighted. Interested readers can refer to the original papers for further details.

3.1. Walkway shaping

The walkway width B varies along the footbridge span according to the following considerations: i. the walkway width at both the span ends remains unchanged because of design constraints, that is, $B(0) = B(L) = B_0$; ii. in order to optimize the effects of the variation of B on the structural response (i.e. on the modal force), $B(x)$ is set proportional to

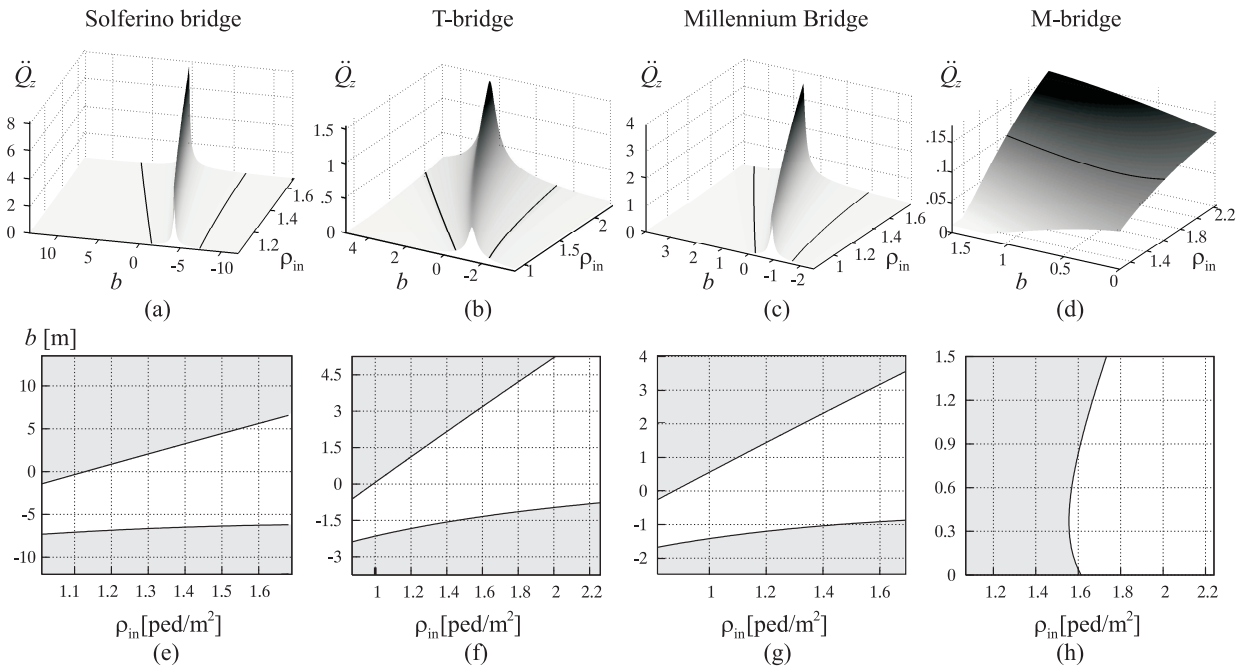

Figure 3: (a)-(d) $\ddot{Q}_z$ versus b and ρ_{in} and (e)-(h) $\ddot{q}_{z,\text{lim}}$ iso-contours in the $\rho_{\text{in}} - b$ plane for the four footbridges

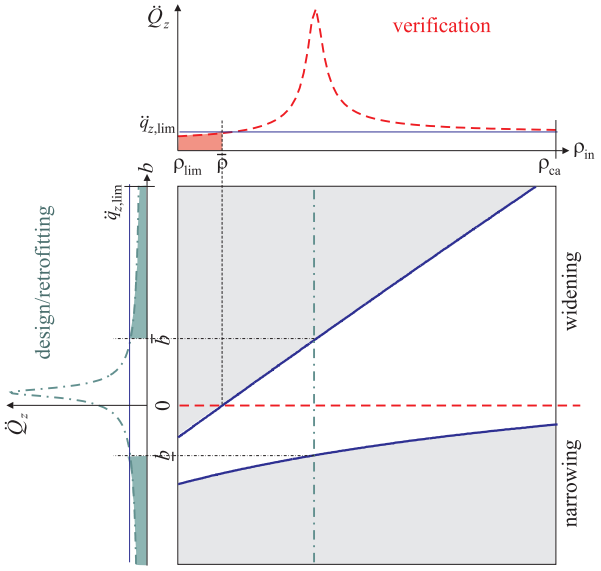

Figure 4: Sketch of the design/verification chart

the eigenvector of the modes of interest $\varphi_i(x)$. For sake of simplicity, in the following a single mode is retained in the walkway shaping, that is, the mode whose frequency is the nearest to the average lateral walking frequency (around 1 Hz). The single-mode shaping is justified in practice because human-induced dynamic response of most footbridges is mainly due to a single mode. Therefore, $B(x)$ is expressed as follows (Fig. 6):

$$B(x) = B_0[1 + b/B_0\ \varphi(x)]. \tag{15}$$

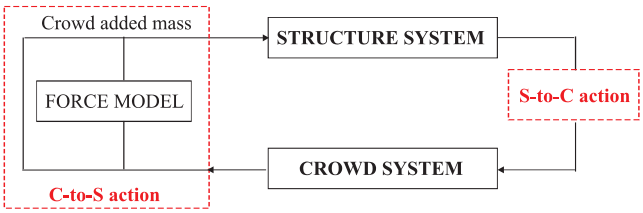

Figure 5: Scheme of the CSI model

It is worth noting that such a shaping is smooth along the span, so that a macroscopic model of the crowd is allowed.

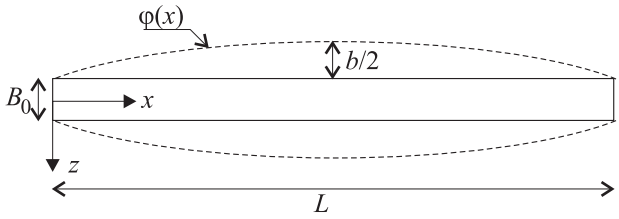

Figure 6: Sketch of the walkway shaping

Otherwise, geometrical features of the walkway having a characteristic length of the same order of magnitude of the pedestrian body (e.g., sharp narrowing or widening, or punctual obstacle along the walkway) would require a microscopic model of each pedestrian (e.g., in [23]) or a multiscale model [35].

3.2. Crowd model

In the presence of crowd-structure interaction and/or variable walkway width, the crowd density is no longer homogeneous along x, and its distribution cannot be approximated by the simple expression (2). Hence, the Crowd dynamics is described by a one-dimesional (1D) first-order macroscopic model, governed by the mass conservation equation. The latter is accompanied by a phenomenological relation that links the crowd mean velocity v to the crowd density ρ and the envelope of the lateral acceleration of the deck $\tilde{\ddot{q}}_z$ [24]:

$$\begin{cases} \dfrac{\partial \rho}{\partial t} + \dfrac{\partial}{\partial x}(\rho v) = 0, \\ v = v[\rho, \tilde{\ddot{q}}_z] = v(\rho) \cdot g(\tilde{\ddot{q}}_z), \end{cases} \tag{16}$$

where $v(\rho)$ is derived according to Eq. (3). The function $g(\tilde{\ddot{q}}_z)$ models the S-to-C action, that is, the reduction of the walking velocity due to the lateral motion of the footbridge deck. Specifically, $g(\tilde{\ddot{q}}_z \leq \ddot{q}_{z,\mathrm{lim}}) = 1$, since pedestrians do not perceive the oscillations, while $g(\tilde{\ddot{q}}_z > \ddot{q}_{z,\mathrm{lim}})$ linearly decreases to zero when $\tilde{\ddot{q}}_z$ equals the maximum acceleration $\ddot{q}_{z,M} = 2.1$ m/s^2 [34] at which pedestrians are no more able to keep balance and stop walking.

In order to introduce in the 1D model the effects of the variation of the walkway width B, the maximum density in Eq. (3) is expressed as a function of x, as already proposed in [36]. $\rho_M = \rho_M(x)$, where $\rho_M(x)$ should vary with the same law as $B(x)$:

$$\rho_M(x) = \rho_{M,0}[1 + b/B_0\, \varphi(x)]. \tag{17}$$

Moreover, the crowd model is nonlocal in space and time, in the sense that pedestrians are assumed to react to what they see in a stretch of road in front of them with a time delay. The interested reader can refer to [37] for further details.

3.3. Force model

The force model adopted in the detailed approach is a generalization of the one described in Section 2, Eqs. (4)-(9). Here a third force component f_{ps} is added to account for the contribution of the n_{ps} pedestrians synchronized with the structure. Moreover, all the force components vary along the span being a function of the crowd density $\rho(x)$. Hence, the lateral force per unit length exerted by the crowd is given by:

$$\mathrm{f}_z = \mathrm{f}_{ps} + \mathrm{f}_{pp} + \mathrm{f}_s, \tag{18}$$

and the numbers of pedestrians per unit length are redefined as:

$$\begin{aligned} n_{ps} &= \rho B\, S_{ps} \\ n_{pp} &= \rho B\, S_{pp}(1 - S_{ps}) \\ n_s &= \rho B - n_{ps} - n_{pp} \end{aligned} \tag{19}$$

by introducing the pedestrian-to-structure synchronization coefficient $S_{ps}(\tilde{\ddot{q}}_z, \omega_r) = S_{ps}(\tilde{\ddot{q}}_z) \cdot S_{ps}(\omega_r)$:

$$S_{ps}(\tilde{\ddot{q}}_z) = \begin{cases} 0 & \tilde{\ddot{q}}_z \leq \ddot{q}_{z,\mathrm{lim}}, \\ 1 - \exp\left[-2.68(\tilde{\ddot{q}}_z - \ddot{q}_{z,\mathrm{lim}})\right] & \tilde{\ddot{q}}_z > \ddot{q}_{z,\mathrm{lim}}, \end{cases} \tag{20}$$

$$S_{ps}(\omega_r) = \exp\left\{-50 \exp\left[(-20\tilde{\ddot{q}}_z/\pi)\right]\right\}(\omega_r - 1)^2. \tag{21}$$

For further details on the derivation of Eq.s (20)-(21), the interested reader can refer to [4].

The f_{ps} component is phase-locked to the footbridge velocity so that pedestrians introduce positive work [38]:

$$\mathrm{f}_{ps} = n_{ps}\alpha(\tilde{\ddot{q}}_z) G \sin(\omega_s t). \tag{22}$$

Its DLF is expressed as a function of the lateral acceleration of the deck, according to the experimental law proposed in [39]:

$$\begin{aligned} \alpha(\tilde{\ddot{q}}_z) &= 0.145 - 0.1 \exp\left[-(0.45 + 1.5e^{\eta})\, \tilde{\ddot{q}}_z^{\,1.35}\right], \\ \eta &= -0.5\left(\frac{\omega_{pl} - \omega_s}{0.14\pi}\right)^2. \end{aligned} \tag{23}$$

3.4. Structure model

The Structure is modelled as a non-linear three-dimensional damped dynamical system, whose equation of motion can be written as:

$$[m_s + m_c]\, \partial_{tt}\mathbf{q}(\mathbf{x}, t) + \mathscr{C}\partial_t\mathbf{q}(\mathbf{x}, t) + \mathscr{L}\mathbf{q}(\mathbf{x}, t) = \mathbf{f}(\mathbf{x}, t), \tag{24}$$

where $\mathbf{q} = \{q_x, q_y, q_z\}$ is the structural displacement; $\mathbf{x} = \{x, y, z\}$ is the space independent variable, x, y and z being the longitudinal, vertical and transverse axes, respectively; t is the time independent variable; $\mathscr{C}$ and $\mathscr{L}$ are the damping and stiffness operators, respectively; $\mathbf{f} = \{\mathrm{f}_x, \mathrm{f}_y, \mathrm{f}_z\}$ is the applied force. The C-to-S action is splitted into two contributions: first, the overall mass m is given by the sum of the structure and the crowd mass, which in turns depends on the solution of Eq. (16); second, the forcing term $\mathbf{f}$ is a function of the crowd density and, as far as the lateral component f_z is concerned, of the lateral acceleration of the deck (see Eq.s (22)-(23)). It is worth pointing out that an analogy to the inertial term can be easily observed for this force component, so that a sort of overall equivalent mass can be obtained by factorisation of the acceleration-dependent terms. In this work only the lateral force is considered.

4. Application and results

The proposed mitigation measure is applied to an ideal footbridge, which is modelled as an Euler-Bernoulli simply-supported beam in the $x - z$ plane and whose structural parameters are summarized in Table 2. The footbridge is supposed to be located in Europe and mainly crossed for leisure, therefore the crowd parameters assume the following values: $\rho_{M,0} = 6$ ped/m^2, $v_M = 1.18$ m/s and $\bar{\gamma} = 0.245$. On the basis of the structure and crowd parameters of the ideal footbridge, ρ_{in} is chosen in the range [0.76 1.69] ped/m^2 and b varies in the range [-2.5 4] m. First,

Table 2: Ideal footbridge structural parameters

L	100 m
B_0	4 m
m_s	2000 kg/m
EJ	5.187e+10 Nm^2
$\omega_{s,0}/2\pi$	0.8 Hz
ζ	0.005
$\varphi(x)$	$\sin(\pi x/L)$

the design chart is obtained through the simplified criterion (Fig. 7). The lateral acceleration of the deck is below the lock-in threshold $\ddot{q}_{z,\text{lim}}$ only for relatively low values of the incoming crowd density ($\rho_{\text{in}} \leq \bar{\rho} = 0.87$ ped/m^2). Otherwise, mitigation measures are recommended. Two scenarios of incoming crowd density are selected: for $\rho_{\text{in}} = 0.9$ ped/m^2 the design chart suggests that walkway widening is more effective than narrowing to reduce vibrations; the opposite happens for $\rho_{\text{in}} = 1.2$ ped/m^2. It should be noted that the latter value is rather high, close to the one usually recorded on footbridge opening days ($\rho_{\text{in}} \approx 1.4$ ped/m^2 in [1]) or sport events ($\rho_{\text{in}} \approx 1.3$ ped/m^2 in [15]). Second,

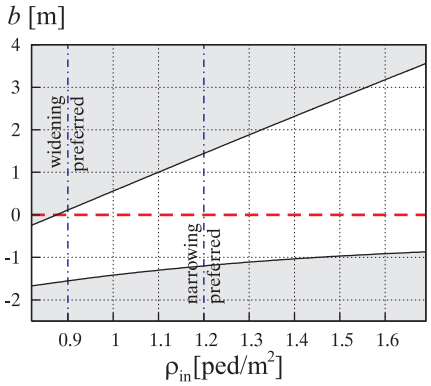

Figure 7: Design chart for the ideal footbridge

computational simulations are performed by means of the CSI model: readers interested in discretization procedures and numerical approach can refer to [24, 37] about structure and crowd systems, respectively. An initial condition of empty footbridge and constant incoming crowd density ρ_{in} are set.

Figure 8 shows an example of the results obtained through a CSI simulation, in the case of $\rho_{\text{in}} = 0.9$ ped/m^2 and original walkway width ($b = 0$). Specifically, the time-space distribution of the crowd density, the time history of the lateral acceleration and the Power Spectral Density (PSD) of the response at midspan are plotted. It can be observed that the crowd density is neither homegeneous in space nor stationary even though the walkway width is constant (Fig. 8a). This is due to the interaction between the crowd and the structure when the acceleration is above the lock-in threshold (Fig. 8b). A steady-state crowd regime can anyway be roughly defined by checking the convergence of the mean value and standard deviation of the number of pedestrians $N(t) = \int_0^L \rho(t)B\,dx$ for increasing length of the sampling window T_n, where $T_1 = 10$ s and $T_{n+1} = T_n + 10$ s. Specifically, the percentage residual on the generic quantity μ is evaluated at the n-th sampling window as $\mu_{res} = |\mu_n - \mu_{n-1}/\mu_n| \cdot 100$. The steady-state regime is considered to be reached when the residual of the first statistical moments is less then 2%. As far as the structural response is concerned, the PSD of the lateral response at midspan over the crowd steady-state regime (Fig. 8c) confirms the main contribution of one mode (highest peak at around 0.75 Hz), while the lower peak at around 0.79 Hz falls in correspondence of the average forcing frequency. Hence, in this case study, the adopted single-mode shaping is confirmed to be perfectly apt to maximize the effects of the variation of B on the modal force.

In order to compare the effectiveness of the countermeasures when b varies, more synthetic results are extracted

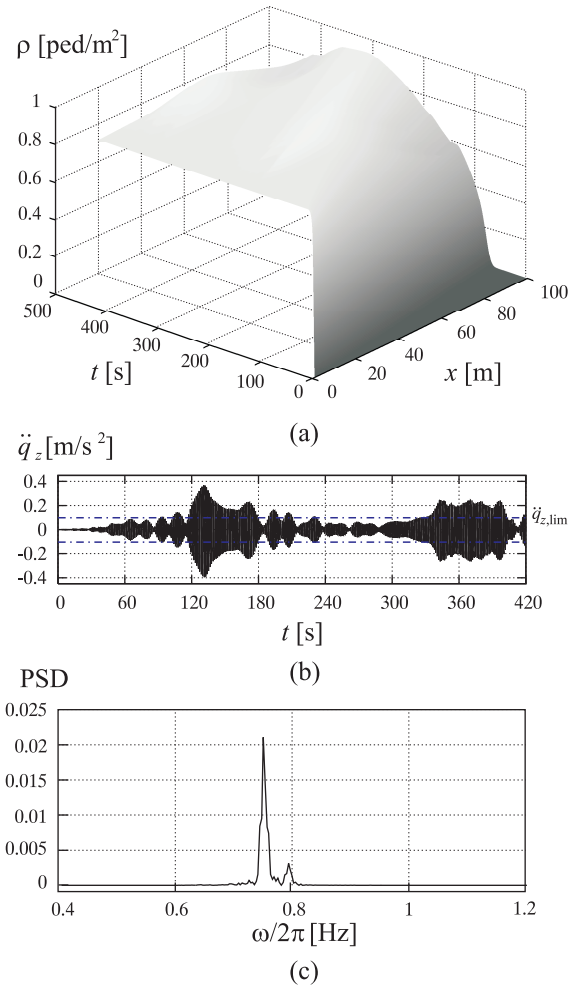

Figure 8: Time-space distribution of the crowd density (a), lateral acceleration (b) and PSD of the response at midspan (c) for $\rho_{in} = 0.9$ ped/m^2 and $b = 0$

in Figure 9 for both incoming crowd scenarios ($\rho_{in} = 0.9$ ped/m^2 left column, $\rho_{in} = 1.2$ ped/m^2 right column). For each of them, both narrowing and widening are evaluated. The results obtained with the strategy suggested by the design chart are highlighted with gray fields. Figures 9a-b and 9c-d plots the time-averaged distribution of the crowd density over the crowd steady-state regime in the case of narrowing and widening, respectively. The crowd density distribution is similar for the cases with constant width $B = B_0$ (red curve): the density increases aroud midspan since pedestrians slow down due to lateral acceleration above $\ddot{q}_{z,\mathrm{lim}}$. In the case of walkway narrowing the bottleneck towards midspan induces the pedestrians to slow down so that a traffic jam (density higher than the capacity one) forms and propagates backwards to the footbridge inlet; pedestrians past the midspan walk faster since they see in front of them the walkway widens. On the contrary, the walkway widening allows the pedestrians before midspan to walk faster so that the density decreases as B increases; past the midspan the density increases towards the outlet, where the deck width narrows, and traffic jam is likely to form the higher ρ_{in} and b are (Fig. 9d).

Figures 9e-f plot the peak value of the lateral acceleration of the deck versus b. First, it can be observed that the trend of the peak accelerations versus b predicted with the simplified model qualitatively agrees with the one obtained through the CSI model. Second, the accelerations obtained with the CSI model are generally higher than

those obtained with the simplified model, due to the strong simplifying assumptions introduced in the latter. Finally, in both incoming crowd scenarios the strategy suggested through the simplified approach (gray squares) turns out to be the most effective in reducing the lateral acceleration.

The efficiency of the mitigation measure has so far been evaluated only from the structural point of view, i.e., looking at the reduction of the lateral acceleration. Neverthless, a footbridge is expected to fullfil other demands concerning its overall in-service performances. In particular, the walkway design should allow the crowd to freely cross the footbridge avoiding congestion and traffic jams. In this perspective, the designer should carefully check that the mitigation measure does not involve a dramatic loss of transportation performances, which are expected to be perturbed when the walkway shape deviates from the straight one (see Fig.s 9a-d). Bearing in mind that a deep analysis of these performances is out of the scope of the paper, a single performance dimensionless metric is introduced here, i.e., the ratio of the time-averaged crowd flow in oulet over the inlet one $(\rho v)_{\text{out}}/(\rho v)_{\text{in}}$. The closer to unit the flow ratio, the smaller the perturbation of the widening/narrowing on the crowd flow. Figures 9g-h plot the flow ratio versus b for each incoming crowd scenarios. It should be noted that the flow ratio is less than unit also for $b = 0$, because crowd-structure interaction reduces the pedestrian velocity (Eq. 16). In general, the variation of the walkway width along the span induces a reduction of the flow ratio with respect to the original value ($b = 0$), due to the increasing tendence to the formation of traffic jams as $|b|$ increases. For the considered values of b, the reduction of the footbridge capacity is always below 25 %, except for $b = 2$ m and $\rho_{\text{in}} = 1.2$ ped/m^2: in this case a dramatic capacity loss is due to the traffic jam ($\rho \cong 5$ ped/m^2) close to the outlet section (Fig. 9d). The rate of reduction of the flow ratio is smaller for both incoming crowd scenarios if the suggested strategy is chosen.

5. Conclusions

In this work, a new approach to the mitigation of human-induced lateral vibrations on footbridges has been proposed, in analogy to aerodynamic countermeasures already successfully employed in Wind Engineering. The countermeasure addresses the passive control of the crowd flow and the applied force in turn, rather than the reduction of the structural response. The control is accomplished by shaping the walkway in plan, in order to modify the pedestrian density, speed and walking frequency. A simplified approach to the preliminary assessment of the footbridge and to the conceptual design of the modified walkway was first proposed, and then a detailed computational analysis was applied to a test-case. The study remains at the proof of concept stage and, in this perspective, only the effects of the countermeasure on the applied load are isolated. Moreover, it should be noticed that the proposed mitigation measure is not effective in an unconstrained walking regime.

The proposed mitigation approach has a number of encouraging aspects. First, it can be included in the early conceptual design of a footbridge, providing a further structural criterion for its shaping in plan. Second, it can be adopted as a retrofitting measure for existing footbridges, if the narrowing of the walkway is considered, e.g., by means of streamlined side barriers. Finally, it is argued to be less expensive and more durable than conventional structural countermeasures based on the increasing of stiffness and damping, respectively.

Some research and development perspectives can be outlined: i. further efficiency proofs can be obtained by means of other modelling approaches (e.g., 2D microscopic pedestrian models) and/or by experimental/in situ measurements; ii. the robustness of the approach (e.g., to account for differing pedestrian traffic conditions) should be further investigated; iii. the possible effects of the mitigation measure on the structural properties (e.g., stiffness, mass) could be taken into account; iv. the mitigation approach could be extended to human-induced vertical vibrations and enriched by a multimode shaping criterion; v. the smooth shaping of the walkway along the span could be replaced and/or integrated by the introduction of punctual obstacles such as walkway equipment (e.g., benches, lighting poles, side barriers) in a retrofitting perspective.

References

[1] P. Dallard, T. Fitzpatrick, A. Flint, S. L. Bourva, A. Low, R. M. Ridsdill Smith, M. Willford, The London Millennium Footbridge, The Structural Engineer 79 (22) (2001) 17–33.

[2] S. Živanović, A. Pavic, P. Reynolds, Vibration serviceability of footbridges under human-induced excitation: a literature review, Journal of Sound and Vibration 279 (2005) 1–74.

[3] V. Racic, A. Pavic, J. M. W. Brownjohn, Experimental identification and analytical modelling of human walking forces: Literature review, Journal of Sound and Vibration 326 (2009) 1–49.

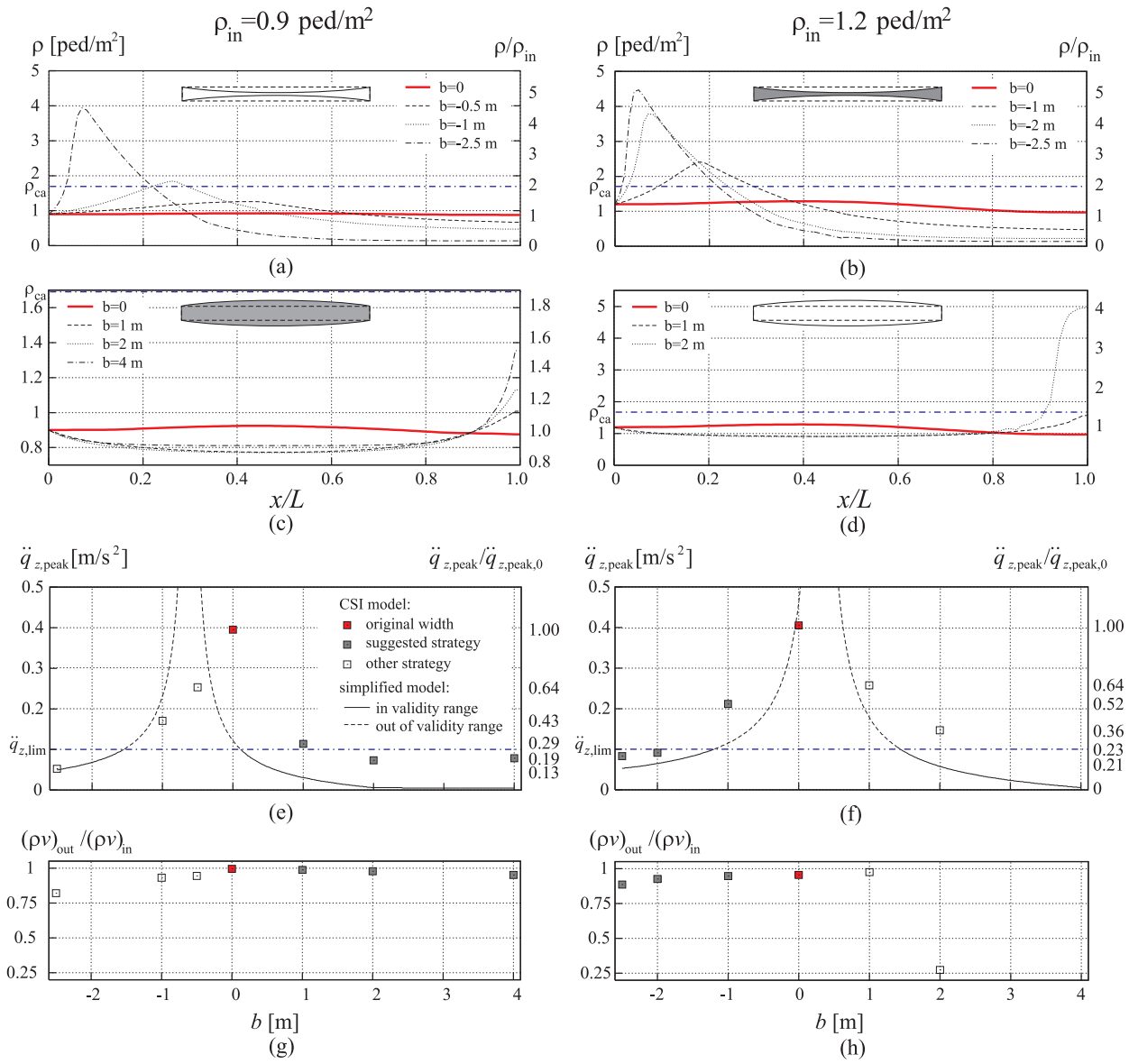

Figure 9: Time-averaged crowd density distributions (a)-(d), peak value of the lateral acceleration (e)-(f) and time-averaged flow ratio (g)-(h) for ρ_{in} = 0.9 ped/m^2 and ρ_{in} = 1.2 ped/m^2

[4] F. Venuti, L. Bruno, Crowd-structure interaction in lively footbridges under synchronous lateral excitation: A literature review, Physics of Life Reviews 6 (3) (2009) 176–206.

[5] A. McRobie, G. Morgenthal, J. Lasenby, M. Ringe, Section model tests on human-structure lock-in, Bridge Engineering 156 (BE2) (2003) 71–79.

[6] A. D. Pizzimenti, F. Ricciardelli, The synchronization: the lessons of the wind engineering and their application to the crowd-structure interaction, in: Proceedings 8th Italian Conference on Wind Engineering, Reggio Calabria, 2004.

[7] D. E. Newland, Pedestrian excitation of bridges, Proceedings of the Institution of Mechanical Engineers, Journal of Mechanical Engineering Science 218c (2004) 477–492.

[8] F. Venuti, L. Bruno, N. Bellomo, Crowd dynamics on a moving platform: Mathematical modelling and application to lively footbridges, Mathematical and Computer Modelling 45 (2007) 252–269.

[9] G. Diana, S. Bruni, A. Collina, A. Zasso, Aerodynamic challenges in super long span bridge design, in: Proceedings International Symposium on Advances in Bridge Aerodynamics, 1998.

[10] A. Kareem, T. Kijewski, Mitigation of motions of tall buildings with specific examples of recent applications, Wind and Structures 3 (2) (1999) 201–251.
[11] C. Jones, P. Reynolds, A. Pavic, Vibration serviceability of stadia structures subjected to dynamic crowd loads: A literature review, Journal of Sound and Vibration 330 (2011) 1531–1566.
[12] S. S. Law, Z. M. Wu, S. L. Chan, Vibration control study of a suspension footbridge using hybrid slotted bolted connection elements, Engineering Structures 26 (2004) 107–116.
[13] E. Caetano, A. Cunha, F. Magalhaes, C. Moutinho, Studies for controlling human-induced vibration of the Pedro e Inês footbridge, Portugal. Part 1: Assessment of dynamic behaviour, Engineering Structures 32 (2010) 1069–1081.
[14] E. Caetano, A. Cunha, F. Magalhaes, C. Moutinho, Studies for controlling human-induced vibration of the Pedro e Inês footbridge, Portugal. Part 2: Implementation of tuned mass dampers, Engineering Structures 32 (2010) 1082–1091.
[15] Y. Fujino, B. M. Pacheco, S. Nakamura, P. Warnitchai, Synchronization of human walking observed during lateral vibration of a congested pedestrian bridge, Earthquake Engineering and Structural Dynamics 22 (1993) 741–758.
[16] P. A. Irwin, Wind engineering challenges of the new generation of super-tall buildings, Journal of Wind Engineering and Industrial Aerodynamics 97 (2009) 328–334.
[17] A. Larsen, S. Esdahl, J. Andersen, T. Vejrum, Storebælt suspension bridge vortex shedding excitation and mitigation by guide vanes, Journal of Wind Engineering and Industrial Aerodynamics 88 (2000) 283–296.
[18] M. W. Sarwar, T. Ishihara, Numerical study on suppression of vortex-induced vibrations of box girder bridge section by aerodynamic countermeasures, Journal of Wind Engineering and Industrial Aerodynamics 98 (2010) 701–711.
[19] S. Bauer, B. Dietmar, N. Seer, Macroscopic pedestrian flow simulation for designing crowd control measures in public transport after special events, in: Proceedings of the 2007 Summer Computer Simulation Conference, San Diego, California, 2007
[20] D. Helbing, A. Johansson, H.Z. Al-Abideen, Dynamics of crowd disaster: an empirical study, Physical Review E 75 (046109) (2007) 1–7.
[21] D. Helbing, I. J. Farkas, P. Molnar, T. Vicsek, Simulation of pedestrian crowds in normal and evacuation situations, in: M. Schreckenberg, S. D. Sharma (Eds.), Pedestrian and Evacuation Dynamics, Springer, Berlin, 2002, pp. 21–58.
[22] D. Helbing, L. Buzna, A. Johansson, T. Werner, Self-organized pedestrian crowd dynamics: Experiments, simulations and design solutions, Transportation Science 39 (2005) 1–24.
[23] S. P. Carroll, J. S. Owen, M. F. M. Hussein, Modelling crowd-bridge dynamic interaction with a discretely defined crowd, Journal of Sound and Vibration 331 (11) (2012) 2685–2709.
[24] L. Bruno, F. Venuti, Crowd-structure interaction in footbridges: modelling, application to a real case-study and sensitivity analyses, Journal of Sound and Vibration 323 (1-2) (2009) 475–493.
[25] Sétra/AFGC, Assessment of vibrational behaviour of footbridges under pedestrian loading (October 2006).
[26] L. Bruno, F. Venuti, A simplified approach for footbridge serviceability assessment under lateral crowd loading, Structural Engineering International 20 (4) (2010) 442–446.
[27] V. Racic , J.M.W. Brownjohn, Mathematical modelling of random narrow band lateral excitation of footbridges due to pedestrians walking. Computers & Structures 90-91 (2012) 116–130.
[28] H. Bachmann, W. Ammann, Vibration in structures induced by man and machines, Structural Engineering Documents, vol. 3e, IABSE, Zurich (1987)
[29] F. Ricciardelli, A.D. Pizzimenti, Lateral walking-induced forces on footbridges, Journal of Bridge Engineering, 12 (6) (2007) 677–88
[30] F. Venuti, L. Bruno, An interpretative model of the pedestrian fundamental relation, Comptes Rendus Mecanique 335 (2007) 194–200.
[31] W. Daamen, Modelling passenger flows in public transport facilities, Ph.D. thesis, Delft University of technology, Department transport and planning (2004).
[32] U. Weidmann, Transporttechnik der Fussgänger, Tech. Rep. n.90, Zürich, ETH (1993).
[33] M. Levavasseur, Modélisation du chargement piétonnier pour passerelles, Master's thesis, Université de Caen Basse-Normandie (2008).
[34] S. Nakamura, Field measurement of lateral vibration on a pedestrian suspension bridge, The Structural Engineer 81 (22) (2003) 22–26.
[35] E. Cristiani, B. Piccoli, A. Tosin, Multiscale modelling of granular flows with application to crowd dynamics, Multiscale Modelling and Simulation 9 (2011) 155 – 182.
[36] M. Delitala, A. Tosin, Mathematical modeling of vehicular traffic: a discrete kinetic approach, Mathematical Models and Methods in Applied Sciences 17 (2007) 901–932.
[37] L. Bruno, A. Tosin, P. Tricerri, F. Venuti, Non-local first-order modelling of crowd dynamics: a multidimensional framework with applications, Applied Mathematical Modelling 35 (2011) 426–445.
[38] C. Butz, M. Feldmann, C. Heinemeyer, G. Sedlacek, B. Chabrolin, A. Lemaire, M. Lukic, P. O. Martin, E. Caetano, A. Cunha, A. Goldack, A. Keil, M. Schlaich, Advanced load models for synchronous pedestrian excitation and optimised design guidelines for steel footbridges (SYNPEX), Tech. Rep. RFS-CR 03019, Research Fund for Coal and Steel (2008).
[39] A. Ronnquist, E. Strommen, Pedestrian induced lateral vibrations of slender footbridges, in: IMAC XXV, Orlando(Florida), 2007.